OLIVER PAJONK, BOJANA V. ROSIĆ,
ALEXANDER LITVINENKO, AND
HERMANN G. MATTHIES

A DETERMINISTIC FILTER FOR NON-GAUSSIAN BAYESIAN ESTIMATION

INFORMATIKBERICHT 2011-04

INSTITUTE OF SCIENTIFIC COMPUTING
CARL-FRIEDRICH-GAUSS-FAKULTÄT
TECHNISCHE UNIVERSITÄT BRAUNSCHWEIG

Braunschweig, Germany

This document was created February 2011 using LaTeX 2_ε.

Institute of Scientific Computing
Technische Universität Braunschweig
Hans-Sommer-Straße 65
D-38106 Braunschweig, Germany

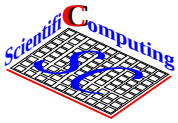

url: www.wire.tu-bs.de
mail: wire@tu-bs.de

A Deterministic Filter for non-Gaussian Bayesian Estimation

Oliver Pajonk, Bojana V. Rosić, Alexander Litvinenko, and Hermann G. Matthies

Institute of Scientific Computing, TU Braunschweig
wire@tu-bs.de

Abstract

We present a fully deterministic method to compute sequential updates for stochastic state estimates of dynamic models from noisy measurements. It does not need any assumptions about the type of distribution for either data or measurement — in particular it does not have to assume any of them as Gaussian. It is based on a polynomial chaos expansion (PCE) of the stochastic variables of the model. We use a minimum variance estimator that combines an a priori state estimate and noisy measurements in a Bayesian way. For computational purposes, the update equation is projected onto a finite-dimensional PCE-subspace. The resulting Kalman-type update formula for the PCE coefficients can be efficiently computed solely within the PCE. As it does not rely on sampling, the method is deterministic, robust, and fast.

In this paper we discuss the theory and practical implementation of the method. The original Kalman filter is shown to be a low-order special case. In a first experiment, we perform a bi-modal identification using noisy measurements. Additionally, we provide numerical experiments by applying it to the well known Lorenz-84 model and compare it to a related method, the ensemble Kalman filter.

Keywords: Bayesian estimation, polynomial chaos expansion, Kalman filter, inverse problem

AMS classification: 60H40, 65M32, 62L12

Contents

1 Introduction

The problem of updating the knowledge of an uncertain quantity in a sequential way from noisy and incomplete data is considered. This is a so-called inverse problem of identification. The goal is to regularise the ill-posed inverse problem by a Bayesian method, which uses a priori knowledge as additional information to the given set of data. For an introduction into the topic, e.g. see Tarantola (2004).

Well established methods for computing Bayesian estimates can be coarsely grouped into two classes: so-called "Linear Bayes" (Goldstein & Wooff, 2007) methods, which update functionals of the random variables (the simplest of which are the Kalman-type methods), and updates based on Bayes's formula itself. The latter ones are usually implemented as sequential Monte Carlo (SMC) methods — also called particle filters (e.g. Gordon et al. (1993)) — or Markov chain Monte Carlo methods (MCMC) (e.g. Hastings (1970)). However, due to the large number of samples required to obtain satisfying results they are computationally quite demanding and hence not very practical. Methods like the Gaussian sum filter (Alspach & Sorenson, 1972) are trying to approximate Bayes's formula. But they, too, tend to have a quite large computational overhead (Houtekamer & Mitchell, 2001).

On the other hand, methods like the extended Kalman filter run into closure problems for non-linear models (Evensen, 1992). Additionally, they are not suitable for high dimensions. Approaching these two problems, the class of Monte Carlo based Kalman-type filters has become quite popular over the last years. The fact that for constant variance the asymptotic rate of convergence of Monte Carlo methods does not depend on the dimension of the sampled space makes these methods applicable to very high dimensional problems, which appear for example in weather forecasting, oceanography, and geophysics. Additionally, these methods naturally allow for non-linear forward models and thus avoid the possibly severe truncation errors coming from linearisation, as they appear for example in the extended Kalman filter.

Kalman-type SMC methods approximate the system covariance matrix, which is central to the Kalman update, by a low-rank estimate from the involved ensemble. Several ensemble-based low-rank methods have been developed since the publication of the original paper describing the ensemble Kalman filter (EnKF) (Evensen, 1994). Most notable are the family of so-called "perturbed observation" implementations (Burgers et al., 1998) and the family of ensemble square-root filters (EnSRF) (Anderson, 2001; Bishop et al., 2001; Whitaker & Hamill, 2002; Tippett et al., 2003). These methods avoid the perturbed observations and thus the sampling errors. For a thorough overview on EnKF and EnSRF see Evensen (2009b). More recent developments include an ODE-based implementation of Bergemann et al. (2009), where the analysis or assimilation solution is computed by numerically integrating a specially crafted ODE. Related methods include the unscented Kalman

filter (Julier & Uhlmann, 2004), which employs a special, deterministic approach instead of Monte Carlo sampling to obtain a second-order correct mean and error covariance estimate — but it also suffers from the curse of dimensionality.

The main idea of this work is to perform a Bayesian update without sampling, but in a direct, purely algebraic way by employing a polynomial chaos expansion (PCE) representation of the involved random variables. The method has been developed as a sequel of ideas presented in (Marzouk et al., 2007; Kučerová & Matthies, 2010). A similar idea has independently appeared in a simpler form in Blanchard (2010) in another context, where it is developed as a combination of polynomial chaos and extended Kalman filter theory. Related approaches include Pence et al. (2010) who combine polynomial chaos theory with maximum likelihood estimation. There, the resulting optimisation problem is solved by gradient descent or a random search algorithm. In contrast, we use a minimum variance estimator based on white noise analysis introduced by Wiener (1938). This kind of estimator is obtained by a simple orthogonal projection of an abstract estimation formula onto a polynomial chaos basis. In the special case when the problem is linear and employs Gaussian random variables the method reduces to the Kalman filter, and in fact the Kalman filter relations are the low-order part of the method.

The polynomial chaos expansion (Wiener, 1938; Ghanem & Spanos, 1991; Holden et al., 1996; Malliavin, 1997; Janson, 1997; Hida et al., 1999; Matthies, 2005, 2008) has already been utilised for the solution of inverse problems, though just for the approximation of the forward problem (Marzouk et al., 2007; Marzouk & Xiu, 2009; Arnst et al., 2010). There, the high computational efficiency of evaluating the PCE solution is employed to estimate the likelihood function from the approximated solution through sampling by an MCMC method. However, this kind of approach is still probabilistic and rather expensive. In order to improve the acceptance probability of proposed MCMC moves, Christen & Fox (2005) have applied a local linearisation of the forward model. However, MC sampling is not the only possible way. For example, (Balakrishnan et al., 2003; Ma & Zabaras, 2009; Li & Xiu, 2009) use a collocation method which samples in a purely deterministic way. This is another way to evaluate the involved integrals. Unfortunately, also collocation needs a fairly high number of sample points when the dimension of the problem becomes large enough.

In this paper we present an efficient numerical strategy for the Bayesian solution of inverse problems. We represent the random variables in the state vector with the help of the PCE (section 2). This representation allows us to use a minimum variance estimate and to directly update the PCE coefficients of the prior state (section 3). In this updating procedure no sampling is involved at any stage. The original Kalman filter is shown to be a special case of the new method (section 4). We then shortly present the ensemble Kalman filter (EnKF) method (section 5) as an

elder relative of our method: they mainly differ in the representation of the involved random variables. By a small numerical example we demonstrate the capability of the described method to update non-Gaussian quantities, after which we apply the EnKF and the described method to the well-known Lorenz-84 model (section 7) and compare the results. Section 8 then concludes our work.

2 Representation of Random Variables

Random variables (RVs) are usually formally defined as measurable functions $r(\omega)$ with values in some vector space $\mathscr{V}$ on a finite measure space with total mass equal to unity. The underlying probability space is given as a triplet $(\Omega, \mathscr{A}, \mathbb{P})$, where Ω is the set of elementary events $\omega \in \Omega$, $\mathscr{A}$ a σ-algebra, and $\mathbb{P}$ the probability measure. In many problems the space Ω is not concretely accessible (and usually is also not really needed, as one may work with the algebra of RVs as primitive objects, e.g. see Segal & Kunze (1978)), so that the usual idea of a function (e.g. given as a formula) looses much of its meaning. The representation of RVs is therefore often strikingly different from what is used for "normal" functions. When propagating a RV through some model, say an evolutionary differential equation, we may recognise some distinctive methods tailored to its representations, which may take the form of:

Sampling: Formally an evaluation of the RV at some — randomly or deterministically — chosen points $\omega_s \in \Omega$. This concept is the simplest as it only needs — usually very many — evaluations of the deterministic model. However, this makes these methods computationally very costly, especially for real applications (e.g. Snyder et al. (2008)).

Distribution: This is the measure $\mathbb{P}_r$ on $\mathscr{V}$ generated by an RV r. For a measurable subset $E \subseteq \mathscr{V}$ one defines $\mathbb{P}_r(E) := \mathbb{P}(r^{-1}(E))$. This description leads to the formulation of conservation equations for the probability, variously known as Kolmogorov-equations, Fokker-Planck-equations, or master equations. For larger models these methods are usually not even contemplated for practical use due to their computational demand (Skorokhod, 1982).

Moments of r: These are the quantities $\boldsymbol{M}_r^{(k)}$ (see Appendix E). This approach leads to — usually ever more complicated — evolutionary integro-differential equations for the moments (Skorokhod, 1982).

Functional approximation: In recent years an alternative representation has gained increasing momentum. The idea is to describe an RV r as a function of other — known — RVs of some simple type. A typical example is

given by polynomials of normalised Gaussian RVs. This is Wiener's polynomial chaos expansion (PCE) (Wiener, 1938; Janson, 1997), also known by a more recent name "white noise analysis" (Holden et al., 1996; Malliavin, 1997; Hida et al., 1999). In some way this representation allows the idea of using the algebra of RVs as primitive objects, and hence it has a distinctly functional analytic flavour (Segal & Kunze, 1978). This representation is the basis of the estimation method described in this paper, so we present now its basic principles.

Let $\{\theta_1(\omega),...,\theta_k(\omega),...\}$ be normalised (zero mean, unit variance) Gaussian RVs (for simplicity we assume real valued scalar RVs), viewed as elements in the space $L_2(\Omega)$ with the inner product

$$\langle\theta_1|\theta_2\rangle_{L_2(\Omega)} = \mathbb{E}(\theta_1(\omega)\theta_2(\omega)). \tag{1}$$

The Gaussian random variables span a subspace

$$\hat{\mathscr{H}} = \text{span}\{\theta_1(\omega),...,\theta_k(\omega),...\} \subseteq L_2(\Omega) \tag{2}$$

which may be completed to a Hilbert subspace $\mathscr{H}$ of $L_2(\Omega)$. Given this structure, we may assume that the RVs $\{\theta_1(\omega),...,\theta_k(\omega),...\}$ are orthonormal or — in other words — uncorrelated. This further means that they form a complete orthonormal system (CONS) for $\mathscr{H}$. In addition, the products of Gaussian RVs from $\mathscr{H}$ are again in $L_2(\Omega)$ as Gaussian RVs possess moments of all orders. The Cameron-Martin theorem (Holden et al., 1996; Malliavin, 1997; Hida et al., 1999) then assures us that the polynomial algebra of these RVs is dense in $L_2(\Omega)$, i.e. we may write any RV as a series of polynomials in variables from $\mathscr{H}$. A convenient choice for an orthogonal generating set are the well-known Hermite polynomials in these Gaussian RVs, given in more detail in Appendix B. Following this, we consider RVs with values in some Hilbert vector space $\mathscr{V}$ with inner product $\langle\cdot|\cdot\rangle_{\mathscr{V}}$. A corresponding inner product in $L_2(\Omega,\mathscr{V})$ is given by

$$\langle\boldsymbol{r}_1|\boldsymbol{r}_2\rangle_{L_2(\Omega,\mathscr{V})} := \mathbb{E}(\langle\boldsymbol{r}_1(\cdot)|\boldsymbol{r}_2(\cdot)\rangle_{\mathscr{V}}). \tag{3}$$

Any RV $\boldsymbol{r} \in L_2(\Omega,\mathscr{V})$ has an expansion in Hermite polynomials — this is the PCE:

$$\boldsymbol{r}(\omega) = \sum_{\alpha\in\mathscr{J}} \boldsymbol{r}^\alpha H_\alpha(\theta_1(\omega),...,\theta_k(\omega),...), \tag{4}$$

where $\mathscr{J} := \mathbb{N}_0^{(\mathbb{N})}$ is a multi-index set (see Appendix A) discriminating the polynomials H_α and coefficients $\boldsymbol{r}^\alpha \in \mathscr{V}$. The sequence of coefficients $(\boldsymbol{r}^\alpha)_{\alpha\in\mathscr{J}}$ — also called the Hermite transform $\mathscr{H}(\boldsymbol{r})$ of the RV $\boldsymbol{r}$, see Matthies (2007) — represents the RV and may be computed simply by projection:

$$\forall\alpha\in\mathscr{J}: \quad \boldsymbol{r}^\alpha = \mathbb{E}(\boldsymbol{r}(\cdot)H_\alpha(\cdot))/\langle H_\alpha|H_\alpha\rangle. \tag{5}$$

Then, one may define the moments of RVs as it is shown in Eq. (E.1). The mean is denoted by $\bar{\boldsymbol{r}} = \boldsymbol{M}_{\boldsymbol{r}}^{(1)}$, and for the covariance between $\boldsymbol{r}_1$ and $\boldsymbol{r}_2$ we write $\boldsymbol{C}_{\boldsymbol{r}_1\boldsymbol{r}_2} = \boldsymbol{M}_{\boldsymbol{r}_1\boldsymbol{r}_2}^{(2)}$ (see Eq. (E.3)). Additionally, $\boldsymbol{C}_{\boldsymbol{r}_1}$ is used as a shorthand for $\boldsymbol{C}_{\boldsymbol{r}_1\boldsymbol{r}_1}$.

For numerical computations the expansion naturally has to be truncated to a finite total polynomial order and limited to a finite number of RVs $\{\theta_1(\omega), ..., \theta_M(\omega)\}$. This may be seen as a "stochastic discretisation". The index α now runs only in some finite set $\mathscr{J}_Z \subset \mathscr{J}$, where Z is defined by the number M of Gaussian RVs and the maximum total order P of the polynomials as

$$Z = (M+P)!/(M!P!). \tag{6}$$

Such a truncated expansion can be used in any model involving the RVs. This is the "ansatz" or trial function. Due to the truncation, the model equation will not be satisfied, but we can use the Galerkin-weighted residual idea to formulate equations for the coefficients $\boldsymbol{r}^{\alpha}$. Formally this means a projection onto the finite dimensional subspace spanned by the H_α with $\alpha \in \mathscr{J}_Z$, by weighting the residual with some test functions — which are often again the Hermite polynomials.

As conclusion, we may now express anything dependent on the RVs through their Hermite transform. At the same time, for the purpose of numerical computation we may project the model onto some finite dimensional subspace, and thus give completely deterministic equations for the coefficients of the PCE.

3 Recursive Estimation for PCE Representations

Let us consider a dynamical system in $\mathbb{R}^n$ whose true state at time t is described by the vector of state variables $\hat{\boldsymbol{x}}_t$. In addition, let Δt be a given time step, such that the state at time $t + \Delta t$ (in notation $t + 1$) may be computed with the help of a known model operator: $\hat{\boldsymbol{x}}_{t+1} = G(\hat{\boldsymbol{x}}_t)$. For notational simplicity let us consider the system at a certain, fixed time $t = T$, which allows us to omit the time index from the following notation.

The true state $\hat{\boldsymbol{x}}$ can be considered as uncertain either because of uncertainty in the initial state, or due to uncertainty in the model G, or both. The goal of the following analysis is the approximate reconstruction of $\hat{\boldsymbol{x}}$ with respect to the previous knowledge and some given data. We assume our prior knowledge to be destilled in an a priori distribution with corresponding random variable $\boldsymbol{x}_f(\omega)$, where the subscript f denotes "forecast". This information shall be combined with the data, obtained by measuring the quantities $\boldsymbol{y}(\omega) \in \mathbb{R}^d$, which depend linearly on the "true" state but are disturbed by a measurement error $\boldsymbol{\varepsilon}(\omega)$, i.e. additive noise:

$$\boldsymbol{y}(\omega) = \boldsymbol{H}\hat{\boldsymbol{x}} + \boldsymbol{\varepsilon}(\omega). \tag{7}$$

Here, $\boldsymbol{H} : \mathbb{R}^n \to \mathbb{R}^d$ denotes the known linear measurement operator. Note that often $d \ll n$, so we deal with an inverse problem that is usually ill-posed in the sense of Hadamard in the deterministic setting (Engl et al., 2000) — but see Stuart (2010) for a mathematical analysis and proof of well-posedness in the stochastic setting. The uncertainty in the measurement error is modelled as an RV, and hence $\boldsymbol{y}(\omega)$ is an RV as well. For simplicity we assume the measurement error to be a centred Gaussian — the method could also deal with other measurement error distributions — so that its description is completely given by the covariance $\boldsymbol{C}_{\boldsymbol{\varepsilon}}$. In addition, we assume that the measurement errors are not correlated with the state forecast, i.e. $\boldsymbol{C}_{\boldsymbol{x}_f\boldsymbol{\varepsilon}} = 0$. The forecast measurement on the other hand is $\boldsymbol{z}(\omega) := \boldsymbol{H}\boldsymbol{x}_f(\omega)$

We assume that all RVs involved are elements of $L_2(\Omega)$, with inner product given by Eq. (1) or Eq. (3). To obtain an improved estimator $\boldsymbol{x}_a(\omega)$ reflecting the prior estimate $\boldsymbol{x}_f(\omega)$ as well as the measurements $\boldsymbol{y}(\omega)$ (with subscript a denoting "analysis" or "assimilated"), a common linear Bayesian approach is to derive a minimum variance estimator using the projection theorem of Hilbert spaces (Luenberger, 1969). In the case of a linear forward model G and purely Gaussian RVs the resulting estimator is well known as the Kalman filter — but note that in the following, linearity of G or the assumption of Gaussian RVs is not needed.

The following theorem presents the minimum variance update when additional data becomes available (Luenberger, 1969):

Theorem 3.1. *Assume that $\boldsymbol{x}_f(\omega)$ is a vector valued random variable which represents an estimator for the unknown $\hat{\boldsymbol{x}}$, and that a measurement $\boldsymbol{y}(\omega)$ becomes available according to Eq. (7). The orthogonal projection $\boldsymbol{x}_a(\omega)$ — in the inner product from Eq. (1) or Eq. (3) and hence the best estimator in the $L_2(\Omega)$ norm — of $\hat{\boldsymbol{x}}$ on the subspace spanned by $\boldsymbol{x}_f(\omega)$ and $\boldsymbol{y}(\omega)$ is given by*

$$\boldsymbol{x}_a(\omega) = \boldsymbol{x}_f(\omega) + \boldsymbol{K}(\boldsymbol{y}(\omega) - \boldsymbol{z}(\omega)), \tag{8}$$

where $\boldsymbol{K}$ is the "Kalman gain" operator

$$\boldsymbol{K} := \boldsymbol{C}_{\boldsymbol{x}_f\boldsymbol{z}} (\boldsymbol{C}_{\boldsymbol{z}} + \boldsymbol{C}_{\boldsymbol{\varepsilon}})^{-1}. \tag{9}$$

If the involved RVs $\boldsymbol{x}_f(\omega), \boldsymbol{x}_a(\omega), \boldsymbol{y}(\omega)$ and $\boldsymbol{z}(\omega)$ are described via Monte Carlo ensembles the resulting method becomes the ensemble Kalman filter (EnKF, see section 5 and Evensen (2009a)). Here we use the PCE instead as representation for the RVs. Namely, we "project the projection formula" Eq. (8) onto the polynomial chaos in order to obtain directly the coefficients of the posterior PCE.

Due to the orthogonality of the polynomial chaos, one may simply project Eq. (8) by multiplying it with each H_α, taking the expectation of the obtained equation and further dividing it by $\|H_\alpha\|^2_{L_2(\Omega)} = \alpha!$ such that for all α :

$$\boldsymbol{x}_a^\alpha = \mathbb{E}(\boldsymbol{x}_a H_\alpha)/\alpha! \tag{10}$$

and so on for $\boldsymbol{x}_f^\alpha, \boldsymbol{y}^\alpha, \boldsymbol{z}^\alpha$ and $\boldsymbol{\varepsilon}^\alpha$. For each α Eq. (8) leads to

$$\boldsymbol{x}_a^\alpha = \boldsymbol{x}_f^\alpha + \boldsymbol{K}(\boldsymbol{y}^\alpha - \boldsymbol{z}^\alpha), \tag{11}$$

or in terms of the Hermite transform

$$\mathscr{H}(\boldsymbol{x}_a) = \mathscr{H}(\boldsymbol{x}_f) + \boldsymbol{K}(\mathscr{H}(\boldsymbol{y}) - \mathscr{H}(\boldsymbol{z})). \tag{12}$$

The simplest representation of Eq. (11) is to collect all the column vectors $\boldsymbol{x}^\alpha$ into a matrix, e.g. $\boldsymbol{X} = [\ldots, \boldsymbol{x}^\alpha, \ldots]$, and with this interpretation the full update simply reads as

$$\boldsymbol{X}_a = \boldsymbol{X}_f + \boldsymbol{K}(\boldsymbol{Y} - \boldsymbol{Z}). \tag{13}$$

This is the final form of the PC updating approach developed in this paper.

4 The Kalman Filter as a Special Case

Let us remark that the term with $\alpha = 0$ in Eq. (11) or Eq. (13) is the update of the mean, thus recovering the well-known Kalman update for the mean (Luenberger, 1969). The same conclusion is reached by taking the expectation of Eq. (8). But the previously mentioned equations also contain the Kalman update for the covariance. For any expansion like

$$\boldsymbol{x}_a(\omega) = \sum_\alpha \boldsymbol{x}_a^\alpha H_\alpha(\omega), \tag{14}$$

the covariance is given by (see Appendix E)

$$\begin{aligned} \boldsymbol{C}_{\boldsymbol{x}_a} &= \mathbb{E}\left((\boldsymbol{x}_a(\cdot) - \bar{\boldsymbol{x}}_a) \otimes (\boldsymbol{x}_a(\cdot) - \bar{\boldsymbol{x}}_a)\right) \\ &= \sum_{\alpha,\beta>0} \boldsymbol{x}_a^\alpha \otimes \boldsymbol{x}_a^\beta \, \mathbb{E}\left(H_\alpha H_\beta\right) \\ &= \sum_{\alpha>0} \boldsymbol{x}_a^\alpha \otimes \boldsymbol{x}_a^\alpha \alpha!, \end{aligned} \tag{15}$$

where $\mathbb{E}\left(H_\alpha H_\beta\right) = \delta_{\alpha\beta}\alpha!$ and $\bar{\boldsymbol{x}}_a = \boldsymbol{x}_a^0$. Employing the matrix representation as in Eq. (13) and introducing the diagonal Gram matrix $(\boldsymbol{\Delta})_{\alpha\beta} = \mathbb{E}\left(H_\alpha H_\beta\right) = \mathrm{diag}(\alpha!)$, one may rewrite Eq. (15) to

$$\boldsymbol{C}_{\boldsymbol{x}_a} = \tilde{\boldsymbol{X}}_a \boldsymbol{\Delta} \tilde{\boldsymbol{X}}_a^T, \tag{16}$$

where $\tilde{\boldsymbol{X}}_a$ is $\boldsymbol{X}_a$ without the $\alpha = 0$ term (the mean). Having $\boldsymbol{C}_{\boldsymbol{x}_f \boldsymbol{\varepsilon}} = 0$, we may tensorise Eq. (13), subtract the mean values and take the expectation of the obtained

equation in order to obtain the covariance:

$$\begin{aligned} \boldsymbol{C}_{\boldsymbol{x}_a} &= \tilde{\boldsymbol{X}}_a \boldsymbol{\Delta} \tilde{\boldsymbol{X}}_a^T \\ &= \left(\tilde{\boldsymbol{X}}_f + \boldsymbol{K}(\tilde{\boldsymbol{Y}} - \tilde{\boldsymbol{Z}})\right) \boldsymbol{\Delta} \left(\tilde{\boldsymbol{X}}_f + \boldsymbol{K}(\tilde{\boldsymbol{Y}} - \tilde{\boldsymbol{Z}})\right)^T \\ &= \boldsymbol{C}_{\boldsymbol{x}_f} + \boldsymbol{K}\boldsymbol{C}_{\boldsymbol{\varepsilon}}\boldsymbol{K}^T + \boldsymbol{K}\boldsymbol{C}_{\boldsymbol{z}}\boldsymbol{K}^T \\ &\qquad - \boldsymbol{C}_{\boldsymbol{x}_f \boldsymbol{z}}\boldsymbol{K}^T - \boldsymbol{K}\boldsymbol{C}_{\boldsymbol{x}_f \boldsymbol{z}}^T \\ &= \boldsymbol{C}_{\boldsymbol{x}_f} + \boldsymbol{K}(\boldsymbol{C}_{\boldsymbol{z}} + \boldsymbol{C}_{\boldsymbol{\varepsilon}})\boldsymbol{K}^T - \boldsymbol{C}_{\boldsymbol{x}_f \boldsymbol{z}}\boldsymbol{K}^T - \boldsymbol{K}\boldsymbol{C}_{\boldsymbol{x}_f \boldsymbol{z}}^T. \end{aligned} \tag{17}$$

Using Eq. (9) one has that

$$\begin{aligned} \boldsymbol{C}_{\boldsymbol{x}_a} &= \boldsymbol{C}_{\boldsymbol{x}_f} + \boldsymbol{C}_{\boldsymbol{x}_f \boldsymbol{z}} (\boldsymbol{C}_{\boldsymbol{z}} + \boldsymbol{C}_{\boldsymbol{\varepsilon}})^{-1} \boldsymbol{C}_{\boldsymbol{x}_f \boldsymbol{z}}^T \\ &\qquad - 2\boldsymbol{C}_{\boldsymbol{x}_f \boldsymbol{z}} (\boldsymbol{C}_{\boldsymbol{z}} + \boldsymbol{C}_{\boldsymbol{\varepsilon}})^{-1} \boldsymbol{C}_{\boldsymbol{x}_f \boldsymbol{z}}^T \\ &= \boldsymbol{C}_{\boldsymbol{x}_f} - \boldsymbol{C}_{\boldsymbol{x}_f \boldsymbol{z}} (\boldsymbol{C}_{\boldsymbol{z}} + \boldsymbol{C}_{\boldsymbol{\varepsilon}})^{-1} \boldsymbol{C}_{\boldsymbol{x}_f \boldsymbol{z}}^T \\ &= \boldsymbol{C}_{\boldsymbol{x}_f} - \boldsymbol{K}\boldsymbol{C}_{\boldsymbol{x}_f \boldsymbol{z}}^T, \end{aligned} \tag{18}$$

which is exactly the update for the covariance estimate from the original Kalman filter (Luenberger, 1969).

Let us point out that in Eq. (11) or Eq. (13) the complete random variable is updated — up to the order kept in the PCE — and not just the first two moments, as it is usually done in the Gauss-Markov theorem — for example in the guise of the Kalman filter (Luenberger, 1969; Jazwinski, 1970).

5 Ensemble Filter Methods

The ensemble Kalman filter can be derived in the same way as the PC updating approach. Thus, in the following we use the same symbols and abbreviations as in section 3. The main difference is that instead of using the Hermite transform of the RVs $\boldsymbol{x}_f(\omega)$, $\boldsymbol{x}_a(\omega), \boldsymbol{y}(\omega)$, and $\boldsymbol{z}(\omega)$ the variables are represented by a set of Monte Carlo samples, here simply called "ensemble": $\boldsymbol{X}_f = [\boldsymbol{x}_f(\omega_1), ..., \boldsymbol{x}_f(\omega_N)]$, and similarly for $\boldsymbol{x}_a(\omega), \boldsymbol{y}(\omega)$, and $\boldsymbol{z}(\omega)$. Each ensemble is conveniently written in matrix form, with one sample in each column. This is in contrast to the matrices of PCE coefficients in Eq. (13).

Consider the ensemble $\boldsymbol{X}_f$ representing the RV $\boldsymbol{x}_f(\omega)$. Each ensemble member has independently been transformed through the (possibly non-linear) forward model. The goal is, given a measurement $\boldsymbol{y}$, to compute a new ensemble $\boldsymbol{X}_a$ conditioned on this measurement. Theorem 3.1 shows that applying the Kalman update Eq. (8) to each ensemble member separately results in an ensemble which has the required statistics.

Conveniently, all necessary covariances to compute the Kalman update can be approximated from the forecast ensemble. For this first centralize $\boldsymbol{X}_f$ and $\boldsymbol{Z}$:

$$\tilde{\boldsymbol{X}}_f := \boldsymbol{X}_f - \bar{\boldsymbol{x}}_f \mathbf{1}_N^T$$
$$\tilde{\boldsymbol{Z}} := \boldsymbol{Z} - \bar{\boldsymbol{z}}\, \mathbf{1}_N^T.$$

Here $\bar{\boldsymbol{x}} := \frac{1}{N}\sum_{i=1}^{N} \boldsymbol{x}(\omega_i)$ denotes the sample mean, and $\mathbf{1}_N^T$ represents a row vector of 1s of length N. Then one may estimate the covariances:

$$\boldsymbol{C}_{\boldsymbol{x}_f \boldsymbol{z}} \approx \tilde{\boldsymbol{X}}_f \tilde{\boldsymbol{Z}}^T \tag{19}$$
$$\boldsymbol{C}_{\boldsymbol{z}} \approx \tilde{\boldsymbol{Z}} \tilde{\boldsymbol{Z}}^T. \tag{20}$$

Note that all normalisation terms $(N-1)^{-1}$ from the covariance matrix estimates may be omitted, as they will cancel out in the update.

As it is very important to treat the measurement $\boldsymbol{y}$ as a random variable (shown in Burgers et al. (1998), but also clear from Eq. (8)), we form a measurement ensemble $\boldsymbol{Y}$ by sampling the measurement RV $\boldsymbol{y}(\omega)$. This RV is typically assumed to be Gaussian with covariance matrix $\boldsymbol{C}_{\boldsymbol{\varepsilon}}$ and mean $\boldsymbol{y}$

$$\forall i = 1, ..., N : \boldsymbol{y}_i \sim \mathcal{N}(\boldsymbol{y}, \boldsymbol{C}_{\boldsymbol{\varepsilon}}). \tag{21}$$

We can now write the EnKF update equation as a special case of Eq. (8) as

$$\boldsymbol{X}_a = \boldsymbol{X}_f + \boldsymbol{K}(\boldsymbol{Y} - \boldsymbol{Z}), \tag{22}$$

where $\boldsymbol{K}$ is again the Kalman gain defined in Eq. (9).

5.1 Implementation Details

Eq. (22) can be implemented almost directly: inserting Eq. (9) into Eq. (22) gives

$$\boldsymbol{X}_a = \boldsymbol{X}_f + \boldsymbol{C}_{\boldsymbol{x}_f \boldsymbol{z}} \overbrace{(\boldsymbol{C}_{\boldsymbol{z}} + \boldsymbol{C}_{\boldsymbol{\varepsilon}})^{-1}(\boldsymbol{Y} - \boldsymbol{Z})}^{=:\boldsymbol{A}}. \tag{23}$$

There are mainly three important points to consider: for numerical stability one should not solve the set of normal equations $\boldsymbol{A} = (\boldsymbol{C}_{\boldsymbol{z}} + \boldsymbol{C}_{\boldsymbol{\varepsilon}})^{-1}(\boldsymbol{Y} - \boldsymbol{Z})$ straightforwardly. Due to possible ill conditioning, it is best solved by pseudo inversion, denoted by $(\cdot)^{\dagger}$, using a singular value decomposition (SVD) (e.g. Evensen (2009a)). For this, we replace $\boldsymbol{C}_{\boldsymbol{\varepsilon}}$ with the ensemble estimate $\boldsymbol{C}_{\boldsymbol{y}}$. This is an acceptable approximation (see Evensen (2003), his section 3.4.3), which comes in handy now:

$$(\boldsymbol{C}_z + \boldsymbol{C}_y)^\dagger = \left(\tilde{\boldsymbol{Z}}\tilde{\boldsymbol{Z}}^T + \tilde{\boldsymbol{Y}}\tilde{\boldsymbol{Y}}^T\right)^\dagger \tag{24}$$

which is, taking into account that $\tilde{\boldsymbol{Z}}\tilde{\boldsymbol{Y}}^T \equiv 0$ and $\tilde{\boldsymbol{Y}}\tilde{\boldsymbol{Z}}^T \equiv 0$,

$$= \left(\left(\tilde{\boldsymbol{Z}} + \tilde{\boldsymbol{Y}}\right)\left(\tilde{\boldsymbol{Z}} + \tilde{\boldsymbol{Y}}\right)^T\right)^\dagger, \tag{25}$$

with the SVD of one factor being

$$\boldsymbol{U}\boldsymbol{\Sigma}\boldsymbol{V}^T = \tilde{\boldsymbol{Z}} + \tilde{\boldsymbol{Y}}. \tag{26}$$

Assume the singular values in the diagonal matrix $\boldsymbol{\Sigma}$ arranged descending by size. Inserting Eq. (26) into Eq. (25) one obtains

$$\left(\left(\tilde{\boldsymbol{Z}} + \tilde{\boldsymbol{Y}}\right)\left(\tilde{\boldsymbol{Z}} + \tilde{\boldsymbol{Y}}\right)^T\right)^\dagger = \left(\boldsymbol{U}\boldsymbol{\Sigma}\boldsymbol{\Sigma}^T\boldsymbol{U}^T\right)^\dagger \tag{27}$$

$$= \left(\boldsymbol{U}\boldsymbol{\Sigma}^\dagger\boldsymbol{\Sigma}^{\dagger T}\boldsymbol{U}^T\right), \tag{28}$$

where $\boldsymbol{\Sigma}^\dagger$ is the pseudo-inverse of $\boldsymbol{\Sigma}$, a diagonal matrix with the inverse of the largest singular values from $\boldsymbol{\Sigma}$. Below a certain threshold in $\boldsymbol{\Sigma}$ the corresponding elements in $\boldsymbol{\Sigma}^\dagger$ are set to zero (Golub & van Loan, 1996). Note that the same solution procedure is used in the PCE-based update Eq. (13).

The second important point is that for the pseudo-inversion to work correctly, all components of the RVs $\boldsymbol{y}(\omega)$ and $\boldsymbol{z}(\omega)$ have to be on the same scale. Otherwise, in the pseudo-inversion, the singular vectors of small scale measurements are systematically associated with small singular values — which obviously are more easily truncated. Thus it could introduce a bias in the update towards large scale measurements. This can be easily fixed by scaling the RVs with the assumed measurement standard deviation, thus making them non-dimensional.

The third important point is that we use second order exact sampling in any case where a random number ensemble $\boldsymbol{\Xi}$ of size N is drawn from an n-dimensional standard normal distribution $\mathcal{N}(0, \boldsymbol{I}_n)$. This may be achieved by subtracting an eventual mean

$$\boldsymbol{\Xi} := \boldsymbol{\Xi} - \bar{\boldsymbol{\xi}}\,\boldsymbol{1}_N^T$$

and correcting the standard deviation of every row $j = 1..n$

$$\forall j : (\boldsymbol{\Xi})_j := (\boldsymbol{\Xi})_j \cdot \left(\sqrt{\mathrm{var}((\boldsymbol{\Xi})_j)}\right)^{-1}$$

of the sample (Evensen, 2004).

6 The Lorenz-84 Model

For the numerical evaluation of the estimation method described in section 3, we consider the well-known "Lorenz-84" model (Lorenz, 1984, 2005). It is described by a set of three state variables $\boldsymbol{x} = (x, y, z)^T$. There x represents a symmetric, globally averaged westerly wind current, whereas y and z represent the cosine and sine phases of a chain of superposed large-scale eddies transporting heat polewards. The state evolution of this model, $\dot{\boldsymbol{x}} = \frac{d\boldsymbol{x}}{dt} = f(\boldsymbol{x}); \boldsymbol{x}(0) = \boldsymbol{x}_0$, is described by the following set of ordinary differential equations (ODEs):

$$\begin{aligned} \frac{dx}{dt} &= -ax - y^2 - z^2 + aF_1 \\ \frac{dy}{dt} &= -y + xy - bxz + F_2 \\ \frac{dz}{dt} &= -z - xz + bxy, \end{aligned} \tag{29}$$

where F_1 and F_2 represent known thermal forcings, and a and b are fixed constants. Given some values for the initial conditions $\boldsymbol{x}_0 = (x_0, y_0, z_0)^T$, this system can be integrated forward in time using, for example, a Runge-Kutta (RK) scheme, as it was done in (Lorenz, 2005; Shen et al., 2010).

The Lorenz-84 model shows chaotic behaviour and is very sensitive to the initial conditions. For this reason we model these as independent Gaussian RVs:

$$\begin{aligned} x_0(\omega) &\sim \mathcal{N}(x_0, \sigma_1) \\ y_0(\omega) &\sim \mathcal{N}(y_0, \sigma_2) \\ z_0(\omega) &\sim \mathcal{N}(z_0, \sigma_3). \end{aligned} \tag{30}$$

Due to the appearance of RVs, the deterministic model Eq. (29) turns into a system of stochastic differential equations (SDEs, Øksendal (1998)), $\dot{\boldsymbol{x}}(\omega) = f(\boldsymbol{x}(\omega)); \boldsymbol{x}(0, \omega) = \boldsymbol{x}_0(\omega)$, with

$$\begin{aligned} \frac{dx(\omega)}{dt} &= -ax(\omega) - y(\omega)^2 - z(\omega)^2 + aF_1 \\ \frac{dy(\omega)}{dt} &= -y(\omega) + x(\omega)y(\omega) \\ &\qquad -bx(\omega)z(\omega) + F_2 \\ \frac{dz(\omega)}{dt} &= -z(\omega) - x(\omega)z(\omega) + bx(\omega)y(\omega), \end{aligned} \tag{31}$$

which needs to be integrated in time to obtain the evolution of the stochastic state vector $\boldsymbol{x}(\omega) = (x(\omega), y(\omega), z(\omega))^T$. To be able to do so one has to choose a representation for the involved RVs.

6.1 Representation by an Ensemble

As mentioned in section 2, one can represent the RVs by Monte Carlo sampling. To approximately solve the SDEs Eq. (31), each of the samples of the initial conditions can be independently integrated forward in time using the deterministic set of ODEs in Eq. (29). At any time t, the set of samples may be used to approximately calculate any statistics for the RVs $\boldsymbol{x}(\omega)$. As this is precisely what ensemble filter methods like the EnKF need, we use the representation by Monte Carlo samples when applying those.

6.2 Representation by PCE

On the other hand, following (Shen et al., 2010) and the mathematical formulation given in section 2, we may readily use the PCE (see Eq. (4) and Eq. (14)) in order to represent the RVs:

$$\boldsymbol{x}(\omega) = \sum_{\alpha \in \mathscr{J}} \boldsymbol{x}^{\alpha} H_{\alpha}(\theta(\omega)). \tag{32}$$

For $\boldsymbol{x}(\omega) = (x(\omega), y(\omega), z(\omega))^T$ denote the Hermite transform of $x(\omega)$ by $\xi := (x^{\alpha})_{\alpha \in \mathscr{J}} = \mathscr{H}(x(\omega))$ (see Appendix D), and similarly by $\eta := (y^{\alpha})_{\alpha \in \mathscr{J}}$ and $\zeta := (z^{\alpha})_{\alpha \in \mathscr{J}}$ the transforms of the $y(\omega)$ and $z(\omega)$ components. The stochastic evolution equation Eq. (31) can then be written in terms of these Hermite transforms.

For computational purposes we have to truncate the Hermite transform, as explained in section 2. Thus, we replace the variables by the approximations $\widehat{\xi}$, $\widehat{\eta}$, and $\widehat{\zeta}$, where $\widehat{\ }$ denotes the projection on the finite subspace generated by $\{H_{\alpha} \,|\, \alpha \in \mathscr{J}_Z\}$. For simplicity we use the same finite subspace for $x(\omega)$, $y(\omega)$ and $z(\omega)$. Of course, now Eq. (31) cannot be satisfied anymore, e.g. the result of a product of two truncated PCEs $\mathrm{Q}_2(\widehat{\xi}, \widehat{\zeta})$ does not necessarily lie in the subspace anymore. To solve this problem we simply do a Galerkin projection onto above subspace. The final result is then the stochastic evolution equation Eq. (31) projected onto the subspace:

$$\begin{aligned}
\frac{d\widehat{\xi}}{dt} &= -a\widehat{\xi} - \widehat{\mathrm{Q}}_2(\widehat{\eta}, \widehat{\eta}) - \widehat{\mathrm{Q}}_2(\widehat{\zeta}, \widehat{\zeta}) + aF_1 e_0 \\
\frac{d\widehat{\eta}}{dt} &= -\widehat{\eta} + \widehat{\mathrm{Q}}_2(\widehat{\xi}, \widehat{\eta}) - b\,\widehat{\mathrm{Q}}_2(\widehat{\xi}, \widehat{\zeta}) + F_2 e_0 \\
\frac{d\widehat{\zeta}}{dt} &= -\widehat{\zeta} - \widehat{\mathrm{Q}}_2(\widehat{\xi}, \widehat{\zeta}) + b\,\widehat{\mathrm{Q}}_2(\widehat{\xi}, \widehat{\eta}),
\end{aligned} \tag{33}$$

where $e_0 := (\delta_{0\alpha})_{\alpha \in \mathscr{J}_Z} = (1, 0, 0, \ldots)$. The terms $\widehat{\mathrm{Q}}_2(\cdot, \cdot)$ denote the truncated/projected PCE of the Hermite transform of the product of two RVs, which

may be computed analytically from the PCEs of the RVs (see Appendix D for details). Now one may integrate Eq. (33) in the same way as in the deterministic case by a RK scheme, for example.

7 Numerical Experiments

We would like to point out that it is our goal to find efficient methods which are able to reliably represent a practitioners "state of information", given all available data (Tarantola, 2004). Following this, in the subsequent numerical experiments we aim to assess and compare the combined uncertainty quantification and state estimation capabilities of the methods. Thus we cannot simply evaluate how closely some specific functional of the RV representation of a method — e.g. the mean or median — resembles the "truth". We have to evaluate and compare the variance that is captured by the different methods — especially in the presence of a non-linear model like Lorenz-84.

7.1 Bimodal Identification

First we would like to show that with the PC updating method it is quite easy to treat non-Gaussian RVs in the update. For this, one has to include non-zero higher order terms into the PCE representing the measurement, $\boldsymbol{Y}$, and include this into the computation of the Kalman gain Eq. (9) and the update Eq. (13).

There are two possibilities to obtain these higher order terms: either one assumes a likelihood and sets the PCE coefficients accordingly (as done with the Gaussian likelihood for the subsequent Lorenz-84 example), or one makes repeated measurements of the "truth" and computes a PCE directly from them — "sampling the truth", so to say.

We demonstrate the second variant using a simple example. We create a PCE of a bi-modal, stationary, scalar "truth" (for simplicity there is no dynamic model involved in this experiment). We assume that we can make repeated measurements of this "truth" which are disturbed by Gaussian noise. For the prior we take, assuming to lack better knowledge, a Gaussian distribution with a large variance and mean zero.

In Fig. 1 – 3 some results of this experiment are shown. The continuous probability density function (pdf) estimates have been obtained by applying a kernel density technique (Botev et al., 2010) to a random sample of the RV. Remember from Eq. (4) that the arguments of the PCE are uncorrelated, standard normal RVs $\{\theta_1, ..., \theta_M\}$ — which are easy to sample. By inserting one such sample into the PCE, we obtain a sample of the RV represented by the PCE. Sampling the PCE is

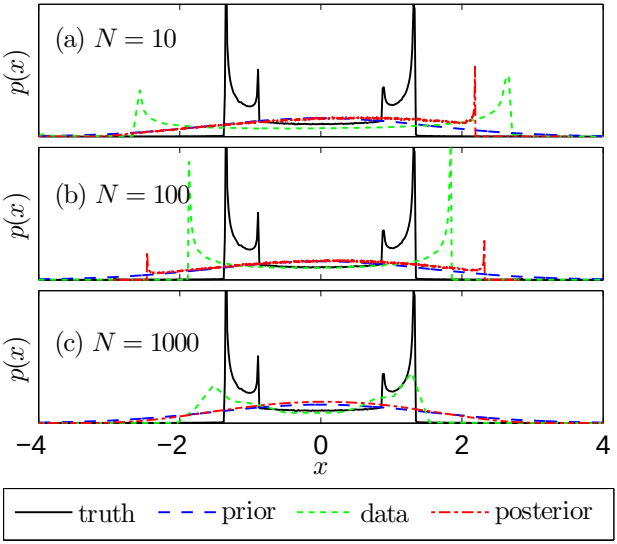

Figure 1: Bi-modal identification experiment after 1 update. Here are shown the results for different amounts of measurements used to determine the PCE coefficients $\boldsymbol{Y}$. First, we use 10 measurements (a), then 100 (b) and finally 1000 (c). The plot contains the truth, the prior and the posterior, as well as the last used measurement as an example.

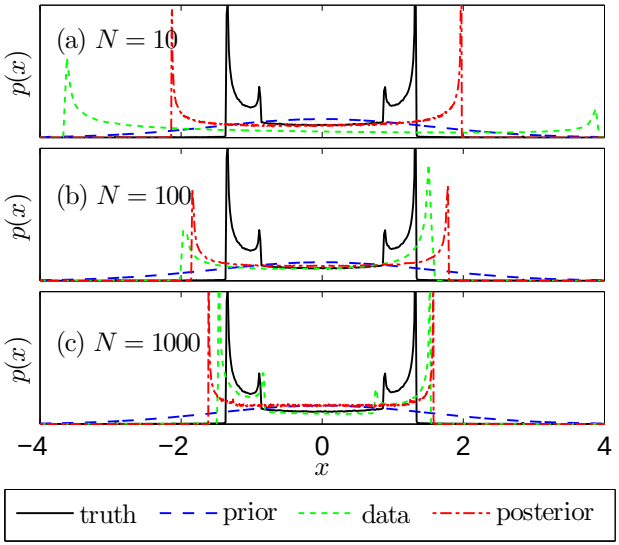

Figure 2: Bi-modal identification experiment after 10 updates (for details see Fig. 1).

computationally rather cheap as it only involves the repeated evaluation of polynomials. However, the sampling is not part of the updating method and only needed to show the results. The same method is used throughout the paper to obtain continuous pdf estimates.

Going back to Fig. 1 one may see that after a single update the prior significantly dominates the posterior in all cases — as it is expected. But after just 10 updates, one may see in Fig. 2 that the posterior already has some resemblance of the "truth" in all cases. The quality, of course, improves with an increased amount of measurements used to determine $\boldsymbol{Y}$. After 100 updates, we can see in Fig. 3 that the posterior quite significantly resembles the "truth" for 100 and 1000 measurements.

However, it is interesting to see that the posterior in the top plot of Fig. 3 is clearly worse than the corresponding one in Fig. 2 — despite of the tenfold increase in total measurements. Hence we can conclude that there is a trade-off involved where to "spend" the available measurements: on one hand, we have to use some updates to suppress the strong influence of the prior — but on the other hand we should use as many measurements as possible to determine the coefficients $\boldsymbol{Y}$ exactly enough.

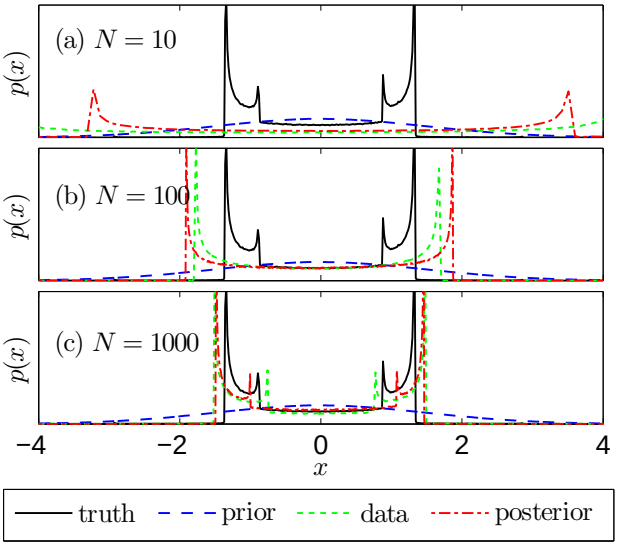

Figure 3: Bi-modal identification experiment after 100 updates (for details see Fig. 1).

7.2 The Lorenz-84 Model

We now apply the PC updating method to a dynamic identification experiment, where it is compared to an ensemble assimilation method. Note that it is currently not clear whether EnKF with perturbed observations or EnSRF with so-called "random rotations" is better suited for the assimilation of data into a non-linear model such as the Lorenz-84 model described in the previous section (Evensen, 2009b). For this study we choose the EnKF with perturbed observations, as described in section 5.

In this numerical experiment the Lorenz-84 system is used in a hidden Markov model setting (see, e.g., Ephraim & Merhav (2002)) as described in section 3. The initial condition of the "unknown truth" is $\hat{\boldsymbol{x}} = (1.0, 0.0, -0.75)^T$, the thermal forcings are set to $F_1 = 8.0$ and $F_2 = 1.23$, and the parameters are set to $a = 0.25$ and $b = 4.0$ (values taken from Lorenz (2005)). Let us point out that F_1, F_2, a, and b are assumed to be known exactly and are used in the forward integration of the "truth" and of the estimates. The noisy measurements of the "truth" are simulated by taking the full state vector (thus in this case $\boldsymbol{H} = \boldsymbol{I}_3$) and adding samples of zero-mean Gaussian noise with known covariance $\boldsymbol{C}_{\boldsymbol{\varepsilon}} = \sigma^2 \boldsymbol{I}_3$

$$\boldsymbol{y}(\omega) = \boldsymbol{H}\hat{\boldsymbol{x}} + \mathcal{N}(0, \boldsymbol{C}_{\boldsymbol{\varepsilon}}). \tag{34}$$

The measurement standard deviation is chosen to be $\sigma := 0.1$, which is approximately 2.5% – 3% of the maximum absolute values that the Lorenz-84 model takes. The initial conditions are chosen as $x_0 = y_0 = z_0 = 0.0$ and $\sigma_1 = \sigma_2 = \sigma_3 = 1.0$ in Eq. (30), starting off with a fairly large initial uncertainty. We use the common choice of integration method for Lorenz-84, a Runge-Kutta scheme of order 4 with a time step of $\Delta t = 0.05$, which corresponds to 6 hours in the model time scale (Shen et al., 2010; Lorenz, 2005).

7.2.1 Assimilation Example

In Fig. 4 a short integration and assimilation example of the PC updating method applied to Lorenz-84, using a PCE of order 3 as was used in Shen et al. (2010), is shown. The plot contains the "truth", as well as some percentiles $p_c := \inf\{x \in \mathbb{R} : \Pr.(x) \geq c/100\}$ estimated from the PCE using sampling. Every 10 days a measurement is assimilated, until day 90. In Fig. 4, one can see how the initial uncertainty is non-linearly transformed until day 10, where the first correction takes place. After three assimilations, the "truth" is quite well followed by p_{50} until day 50, where an outlier measurement or a highly unstable regime of Lorenz-84 makes p_{50} divert from the truth. However, note that the "truth" is still quite well embedded between p_5 and p_{95}. After the measurements at day 60 and 70, the "truth" is tracked quite well again by p_{50} and the uncertainty reduces.

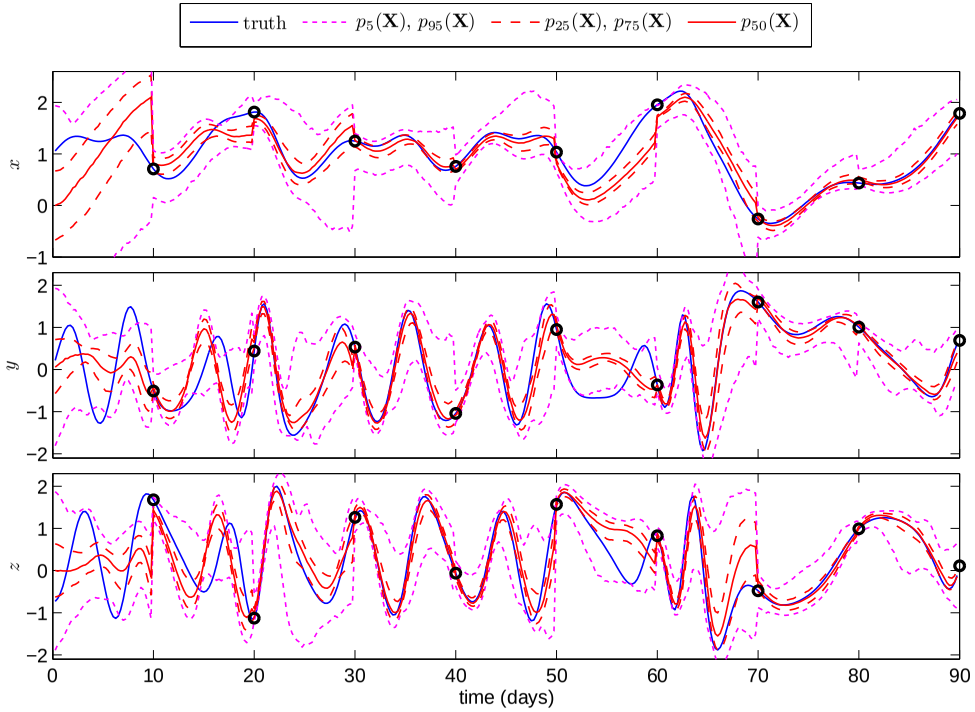

Figure 4: Example of the PC updating method applied to the Lorenz-84 model. The black circles mark the assimilation time points (every 10 days). Here it is plotted, for all dimensions x, y, z of the model, the "truth" and some percentiles estimated from the PCE $\mathbf{X}$ using sampling ($p_5, p_{25}, p_{50}, p_{75}$ and p_{95}).

From this experiment one may learn how the method is working in principle, and that it is able to represent and update skewed distributions: this can be seen by looking at the sometimes quite asymmetric structure of the symmetrically chosen percentiles before and also after the updates.

7.2.2 Percentile Estimation

Here it is investigated how different percentile estimates of the PC updating method compare to an EnKF by the following experimental setup: the previously mentioned initial conditions are integrated for 10 days before the first update to allow for some non-linear mixing. Then, starting at $t = 10$ days, updates with noisy measurements are performed every 2 days, until a total integration of 190 days has occurred (so the data assimilation runs for 180 days). We compute statistics of our results over 1000 runs of the same experiment in order to assess effects that come from the specific values of the simulated measurement error in Eq. (34). The pseudo random number generators used to generate the measurement noise, as well as the initial and measurement ensemble for the EnKF, are initialized differently for each of these runs, of course.

Fig. 5 shows a comparison of the PC updating method to the EnKF. We show the "truth" and the mean of some percentiles estimated from the PCE, as well as from the EnKF-ensemble. For the EnKF we chose an ensemble size of 20 because the forward simulation of 20 ensemble members using Eq. (29) has a similar computational load as the stochastic forward simulation using Eq. (33), as the PCE of order 3 in 3 independent RVs has 20 terms (see Eq. (6)). However, the plots for ensemble sizes of, e.g., 40 and 80 do not differ noticeably. On the plot one can see that after some updating, the p_{50} estimates quite closely follow the truth for both methods. The p_{25} and p_{75} estimates encompass the truth, though we see some minor misjudgements of the EnKF around $t = 120$, $t = 160$, and $t = 180$. Note that the EnKF generally estimates a lower variance than PC updating, as can be clearly seen when comparing the p_5 and p_{95} estimates. The minor misjudgements of the EnKF as well as the lower estimated variance suggest that an ensemble of size 20 is not sufficient to capture the uncertainty involved in this experimental setup — the p_{50} estimate may quite well resemble the truth, though.

7.2.3 Variance Estimation

In this experiment we compare the mean of the relative variance estimated from the PCE and the EnKF across different PCE orders $P = 1, 2, 3$ and ensemble sizes $N = 20, 40, 320$. The mean has been computed from 1000 repetitions of the same experiment, like before. For comparison the variance of the p_{50} estimate is included in all plots. It has been computed from the same 1000 repetitions. All estimates

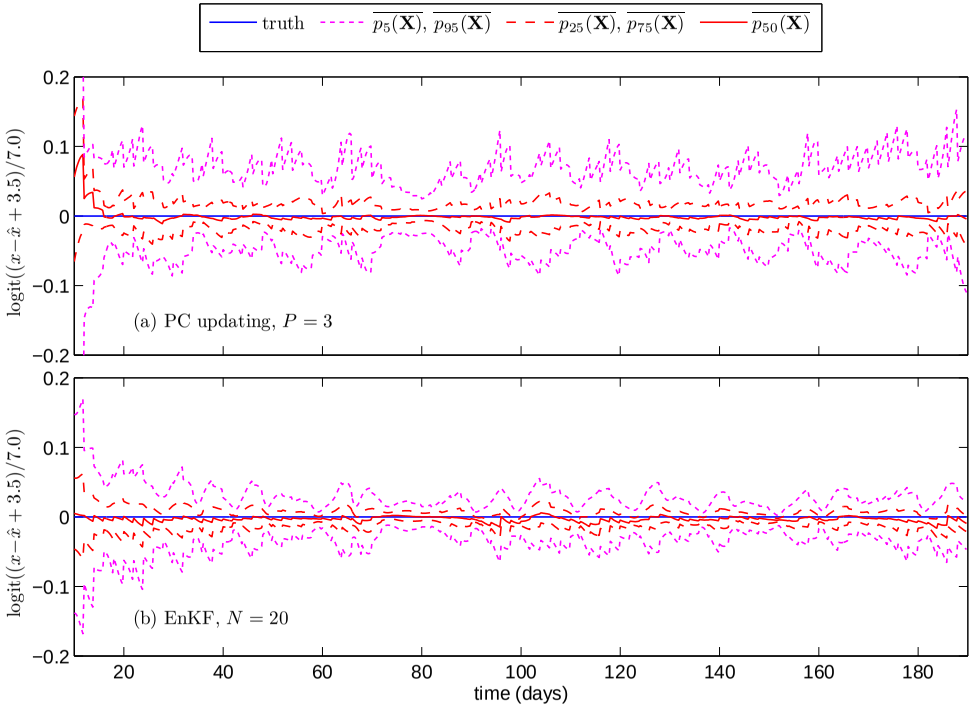

Figure 5: Comparison of the PC updating method to the EnKF, applied to Lorenz-84. Here it is plotted, only for the first dimension x of the model, the "truth" and the mean of some percentiles estimated from the (a) PCE and (b) EnKF-ensemble $\mathbf{X}$ ($p_5, p_{25}, p_{50}, p_{75}$ and p_{95}). The mean has been computed over 1000 runs of the same experiments. The vertical axis has been centred to $\hat{x}$ and scaled with the logit function for clarity. Note that the plotting starts with the first update at $t = 10$ days.

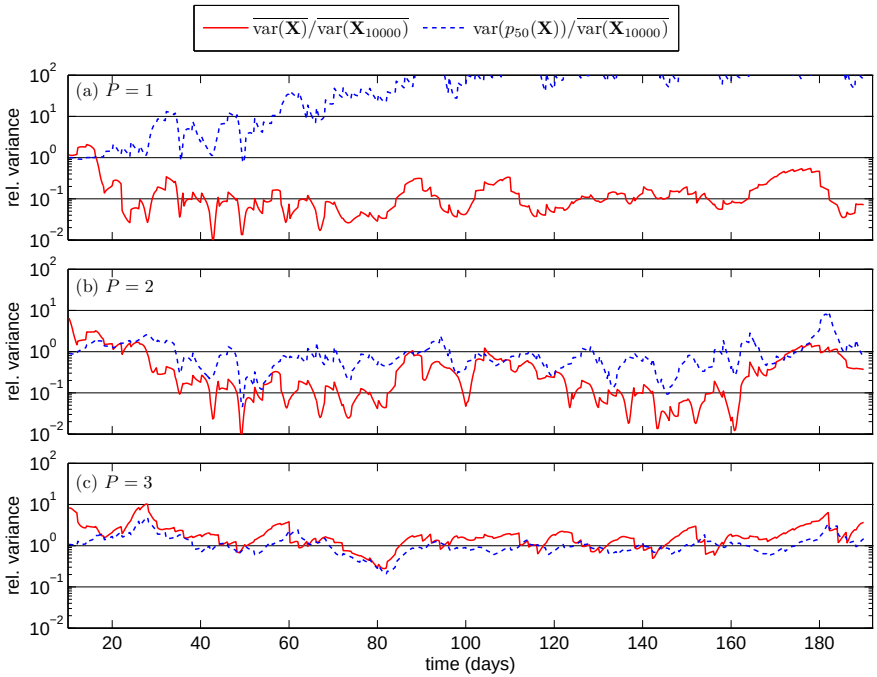

Figure 6: Comparison of the relative variance estimation of the PC updating method for different orders of the PCE. Here it is plotted, only for the first dimension x of the model, the relative mean variance of the PCE, which has been computed from 1000 random repetitions of the same experiment. It is compared to the relative variance of the p_{50} estimate, which has been computed from the same 1000 repetitions. The p_{50} estimate is obtained from the PCE using sampling. Everything is plotted relative to the mean variance computed from 1000 repetitions of the same experiment using EnKF and an ensemble size of 10000.

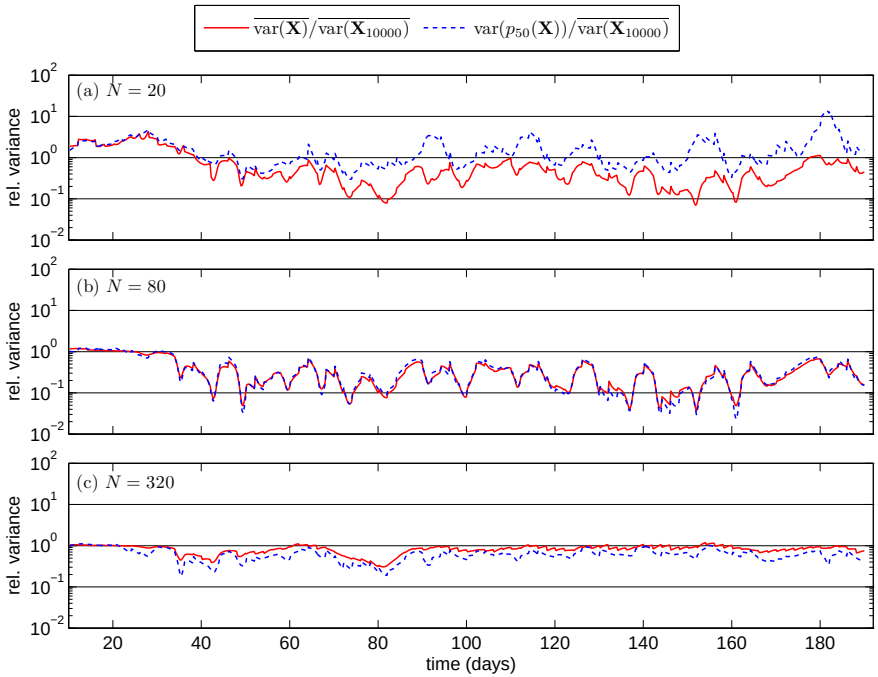

Figure 7: Comparison of the relative variance estimation of the EnKF for different ensemble sizes. Here it is plotted, only for the first dimension x of the model, the relative mean variance of the ensemble, which has been computed from 1000 random repetitions of the same experiment. It is compared to the relative variance of the p_{50} estimate, which has been computed from the same 1000 repetitions. The p_{50} estimate is obtained directly from the ensemble. Everything is plotted relative to the mean variance computed from 1000 repetitions of the same experiment using EnKF and an ensemble size of 10000.

in this experiment are plotted relative to a reference variance obtained from 1000 repetitions of an EnKF run with 10000 ensemble members. This we consider "large enough", as the variance estimates obtained from the same experimental setup, but with "just" 640 ensemble members, are almost the same.

One may see in Fig. 6 (a) that for polynomial order 1, PC updating is unable to maintain a stable p_{50} estimate — it even goes out of the plotted scale. This is to be expected, as the PCE has only 4 terms (see Eq. (6)) and not enough variance is captured. The variance estimate is also quite unstable and is occasionally two orders of magnitude smaller than the reference variance. For polynomial order 2, shown in Fig. 6 (b), the estimated variance is not much different, except for the time interval $t \in [120, 170]$ days. The variance of the p_{50} estimate is significantly reduced and comes much closer to the estimated variance. Thus, the results for polynomial order 2 are better than for 1 but not what one would call reliable. However, already for polynomial order 3, shown in Fig. 6 (c), the variance estimate is significantly higher, more stable, and much closer to the reference variance estimate. Additionally, the variance of the p_{50} is almost never underestimated.

To compare these results with the EnKF, Fig. 7 shows the same plots as Fig. 6 for selected ensemble sizes. In Fig. 7 (a) one may see the often mentioned behaviour of the EnKF to underestimate the variance after some updating: for 20 ensemble members the variance of the p_{50} estimate is quite well estimated up to 40 days, where it starts to drop. Remember that Fig. 7 (a) loosely corresponds to Fig. 6 (c) from a computational load perspective. There, the variance is not dropping after some time and is generally larger than for the EnKF. Even quadrupling the ensemble size to 80, shown in plot Fig. 7 (b), does not change the variance estimate significantly. Interestingly, the variance of the p_{50} estimate drops to almost precisely the estimated variance over the whole assimilation period. Finally, Fig. 7 (c) shows a "huge" ensemble of 320, where we can see the start of the convergence to the 10000 ensemble member run. The variance is still consistently underestimated, but much less than in the other cases. Additionally, the variance of the p_{50} estimate drops consistently below the mean variance estimate.

Comparing Fig. 6 (c) with the other plots in Fig. 6 and Fig. 7, we can see that the PC updating estimates a variance that is closer to the 10000-member EnKF run than all other experiments — except the "huge" 320-member EnKF run, which is, of course, to be expected. Over most of the assimilation period it is even quite consistently larger than the reference variance. This may be a result of the fact that the PC updating, due to the orthogonality of the involved expansion, is more easily able to handle non-Gaussian RVs. The EnKF ensemble is not orthogonal — though some promising approaches have been made in, for example, Evensen (2004) — and the initial span is even getting smaller during the forward integration and updating as the ensemble members become more and more dependent (e.g. see

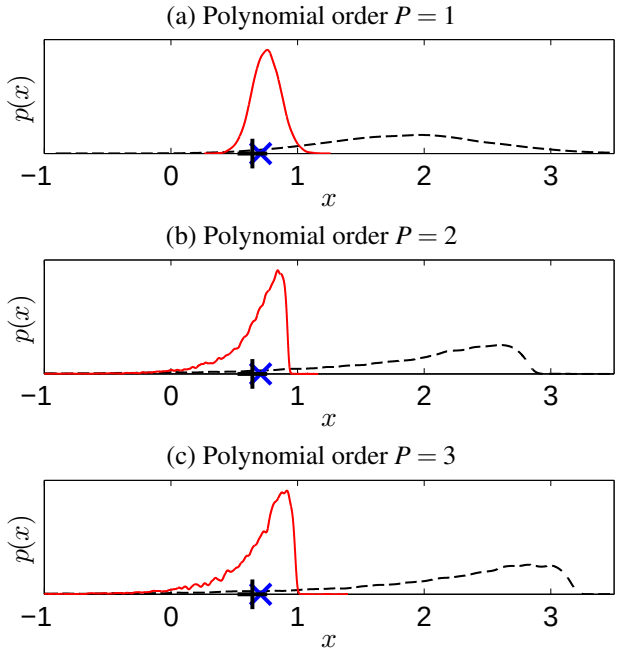

Figure 8: Probability density estimates for the first PC update at $t = 10$ days of the first dimension x of Lorenz-84. The dashed, black line is the prior; the solid, red line is the posterior; the blue $\times$ symbol is the value of the truth; the green $+$ symbol is the value of the noisy measurement.

Houtekamer & Mitchell (2001)). Thus, the EnKF needs a comparably large amount of ensemble members to span and maintain spanning the same subspace as PC updating. There, no special steps to maintain orthogonality have to be taken as it is inherent to the method. Following this argumentation, the updating and maintenance of non-Gaussian RVs in the context of the Lorenz-84 model is investigated next.

However, it is important to point out that the reference of a set of EnKF runs with 10000 ensemble members is not representing "the best we can do" in terms of Bayesian updating, so it is not possible to say which method is "better" by this direct comparison. All that can be done is to point out differences.

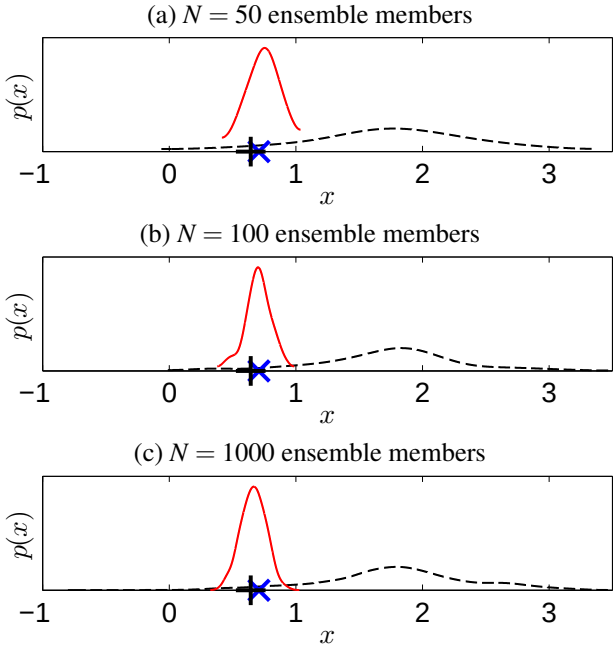

Figure 9: Probability density estimates for the first EnKF update at $t = 10$ days of the first dimension x of Lorenz-84 (legend: see Fig. 8).

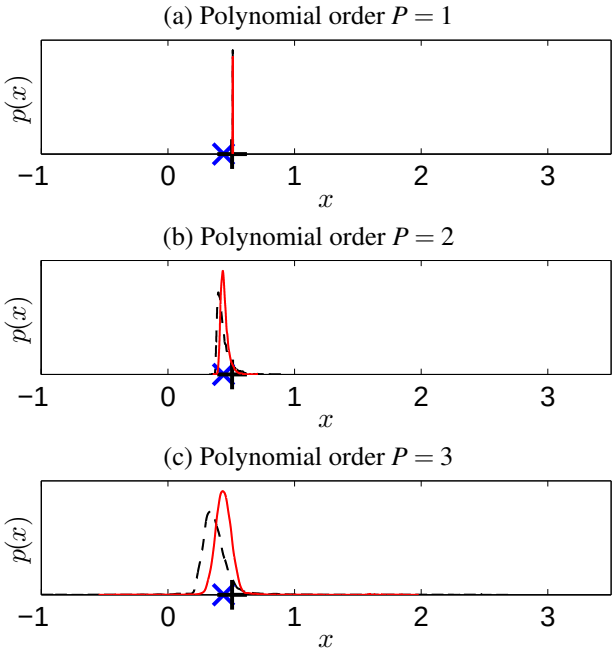

Figure 10: Probability density estimates for the last PC update at $t = 188$ days of the first dimension x of Lorenz-84 (legend: see Fig. 8).

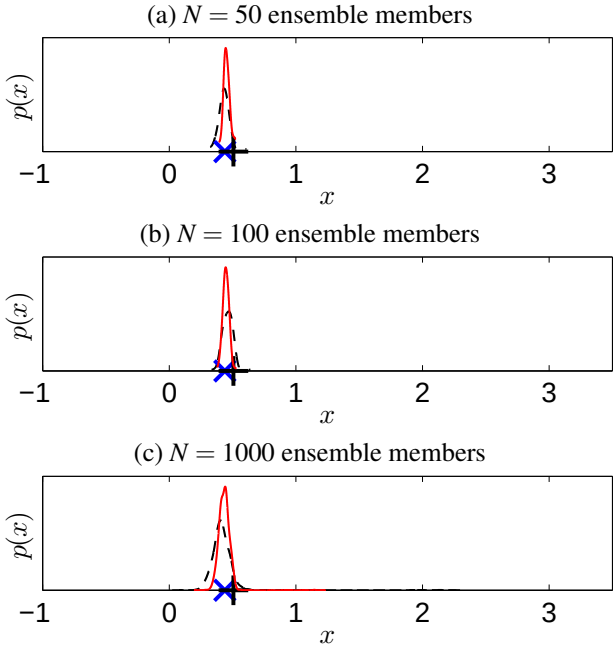

Figure 11: Probability density estimates for the last EnKF update at $t = 188$ days of the first dimension x of Lorenz-84 (legend: see Fig. 8).

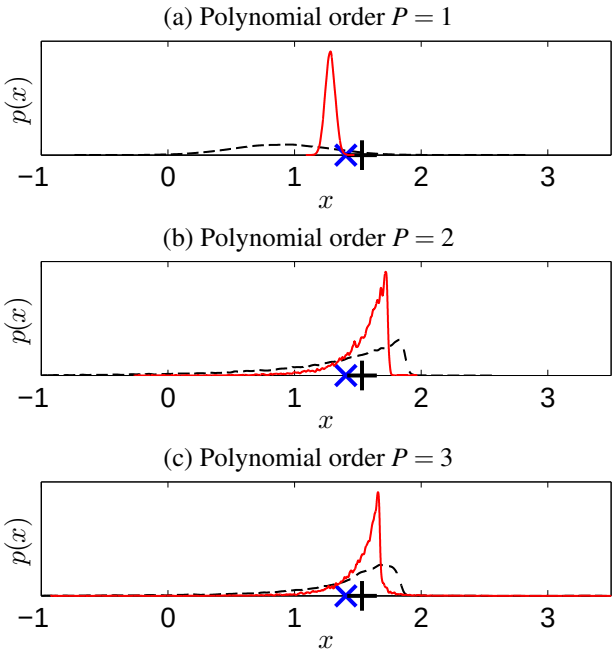

Figure 12: Probability density estimates for the PC update at $t = 110$ days of the first dimension x of Lorenz-84, with a lower assimilation frequency (legend: see Fig. 8).

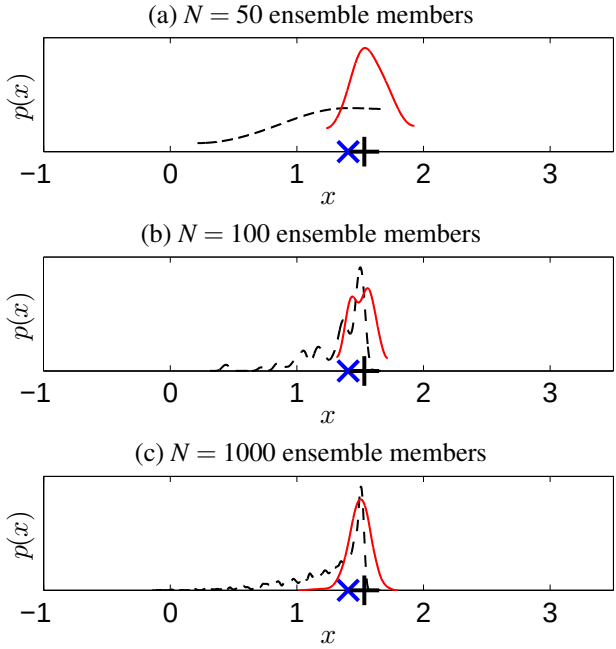

Figure 13: Probability density estimates for the EnKF update at $t = 110$ days of the first dimension x of Lorenz-84, with a lower assimilation frequency (legend: see Fig. 8).

7.2.4 Probability Densities and Updates

Figs. 8 – 11 show pdf estimates for the prior and posterior for both the PC updating method and the EnKF, across different polynomial orders/ ensemble sizes, respectively. For the PCE we have again used Monte Carlo sampling to obtain a continuous estimate of the pdf; for the EnKF, the ensemble itself is the required sample which is used in the mentioned kernel density estimation technique. Note that for this experiment we change the initial conditions to $\sigma_1 = \sigma_2 = \sigma_3 = 0.5$ in Eq. (30) so that the prior in Fig. 8 and Fig. 9 is a bit more pronounced. Note that we perform exactly the same assimilation experiment for both methods, including the specific samples used to disturb the measurements of the truth. Thus, the plots may be directly compared.

In Fig. 8 and Fig. 9 we compare the pdfs for $t = 10$ days, which is the first update. For the PCE representation in Fig. 8, we can see how the prior obtained from integrating the initial conditions for 10 days is quite skewed for polynomial orders 2 and 3. This is to be expected as a PCE of total polynomial order 1 can only represent multivariate Gaussian RVs. For the ensemble representation in Fig. 9, the prior is quite symmetric for 50 ensemble members. For 100 and 1000 members we can see a slighly skewed structure — it is not as pronounced as for the PCE representation with polynomial order 2 or 3, though, and looks more like the one obtained from a polynomial order of 1. The update for both the EnKF and the PC updating is, as expected, moving the mean and reducing the variance. However, the PC updating of orders 2 and 3 is clearly able to retain the skewed structure of the prior. One can also see the convergence of the PCE: with increasing polynomial order more and more details are added. The posterior of the EnKF, on the other hand, looks quite Gaussian, even for an ensemble size of 1000.

At the end of the assimilation period, at $t = 188$ days, one can see in Fig. 10 and Fig. 11 that both methods have almost lost all non-Gaussian structure. Both the prior and the posterior are more or less Gaussian — only for polynomial orders 2 and 3, as well as the ensemble of size 1000, one may percieve a slight skewness. For polynomial order $P = 1$ we can see that the RV has effectively converged to a Dirac delta — which suggests that all variance has been lost and the polynomial order is clearly not sufficient for this experimental setup. However, this loss of non-Gaussian structure may be due to the amount and frequency of Gaussian measurements which have been assimilated into the model.

To investigate the non-Gaussian updating a bit closer we ran the same experiment with a decreased assimilation frequency: data is assimilated only every 10 days, starting at day 10. This results in a longer non-linear mixing between the updates and thus should create pdfs which are more non-Gaussian. The rest of the experiment stays the same. In Fig. 12 and Fig. 13 one may clearly see how the PC updating method retains the non-Gaussian structure of the prior when doing the update, whereas the EnKF eliminates most of it even for a quite large ensemble of

size 1000, where the prior is clearly non-Gaussian. Thus, from an uncertainty quantification perspective, the PC updating analysis contains more information, hinting at possible advantages of this method. Whether the PCE-based method is in some sense superior to the EnKF or not cannot be judged conclusively from this simple experiment, though, and requires further investigation.

Remark Most of the computation operations done in the update procedure are based on standard matrix algebra (BLAS, LAPACK packages). However, in order to speed-up certain computations we have used a tensorial algebra as it is provided in Bader & Kolda (2006).

8 Conclusions

We have developed a method which combines Bayesian updating of uncertainty with the representation of random variables by PCE. The resulting update equation is fully deterministic and thus does not involve any sampling error, as opposed to Monte Carlo methods. However, it involves a truncation error from the truncated PC expansion. The original Kalman filter has been shown to be a low order special case of the new method. The presented method has been employed for the identification of a bi-modal truth. In an additional experiment, the PC updating method has been applied to the recursive identification of uncertain initial values for a chaotic dynamic system, the Lorenz-84 model. On this example it has been compared to a related sequential Monte Carlo technique, the ensemble Kalman filter. Differences and similarities have been pointed out.

The method has shown some appealing mathematical properties, as well as experimental capabilities. It is a promising combination of Bayesian inversion and uncertainty quantification techniques based on the PCE. By numerical experiments we have shown that it is able to handle RVs which have a skewed or even bimodal distribution. However, the update equation is simple and, as the necessary covariance estimates can be directly computed from the PC representation, quite efficient. As the method does not involve any closure assumptions besides the PCE truncation, it is easily applicable to non-linear systems.

It is clear that there are still some problems to solve on the path towards real applications, e.g., to complex geophysical systems. But there is one more thing to consider: the method is fully deterministic, which brings applications in areas into reach which have strong security restrictions or severe real time requirements. There sequential Monte Carlo methods, but also linearity and/or Gaussian assumptions of the original (extended) Kalman filter, may be inadequate.

Acknowledgment

The support of SPT Group GmbH in Hamburg, the Deutsche Forschungsgemeinschaft (DFG) and the German Luftfahrtforschungsprogramm of the Federal Ministry of Economics (BMWA) is gratefully acknowledged.

The following appendices collect some basic properties of the polynomial chaos expansion (PCE), the connected Hermite algebra, and the use of the Hermite transform.

A Multi-Indices

In the PCE formulation, the need for multi-indices of arbitrary length arises. Formally they may be defined by

$$\alpha = (\alpha_1, \ldots, \alpha_j, \ldots) \in \mathscr{J} := \mathbb{N}_0^{(\mathbb{N})}, \tag{A.1}$$

which are sequences of non-negative integers, only finitely many of which are non-zero. As by definition $0! := 1$, the following expressions are well defined:

$$\begin{aligned} |\alpha| &:= \sum_{j=1}^{\infty} \alpha_j, \\ \alpha! &:= \prod_{j=1}^{\infty} \alpha_j!, \\ \ell(\alpha) &:= \max\{j \in \mathbb{N} \,|\, \alpha_j > 0\}. \end{aligned} \tag{A.2}$$

B Hermite Polynomials

As there are different ways to define — and to normalise — the Hermite polynomials, a specific way has to be chosen. In applications with probability theory it seems most advantageous to use the following definition (Hida et al., 1999; Holden et al., 1996; Janson, 1997; Malliavin, 1997):

$$h_k(t) := (-1)^k e^{t^2/2} \left(\frac{\mathrm{d}}{\mathrm{d}t}\right)^k e^{-t^2/2}; \forall t \in \mathbb{R}, k \in \mathbb{N}_0, \tag{B.1}$$

where the coefficient of the highest power of t — which is t^k for h_k — is equal to unity.

The first five polynomials are

$$\begin{aligned} h_0(t) &= 1, \qquad h_1(t) = t, \qquad h_2(t) = t^2 - 1, \\ h_3(t) &= t^3 - 3t, \qquad h_4(t) = t^4 - 6t^2 + 3, \end{aligned}$$

and the recursion relation for these polynomials is

$$h_{k+1}(t) = t\,h_k(t) - k\,h_{k-1}(t); \quad k \in \mathbb{N}. \tag{B.2}$$

These are orthogonal polynomials w.r.t. the standard Gaussian probability measure Γ, where $\Gamma(\mathrm{d}t) = (2\pi)^{-1/2} e^{-t^2/2}\,\mathrm{d}t$ — the set $\{h_k(t)/\sqrt{k!} \,|\, k \in \mathbb{N}_0\}$ forms a complete orthonormal system (CONS) in $L_2(\mathbb{R}, \Gamma)$ — as the Hermite polynomials satisfy

$$\int_{-\infty}^{\infty} h_m(t)\,h_n(t)\,\Gamma(\mathrm{d}t) = n!\,\delta_{nm}. \tag{B.3}$$

Multi-variate Hermite polynomials will be defined right away for an infinite number of variables, i.e. for $\boldsymbol{t} = (t_1, t_2, \ldots, t_j, \ldots) \in \mathbb{R}^{\mathbb{N}}$, the space of all sequences. This uses the multi-indices defined in Appendix A: For $\alpha = (\alpha_1, \ldots, \alpha_j, \ldots) \in \mathscr{J}$ remember that except for a finite number all other α_j are zero; hence in the definition of the multi-variate Hermite polynomial

$$H_\alpha(\boldsymbol{t}) := \prod_{j=1}^{\infty} h_{\alpha_j}(t_j); \quad \forall \boldsymbol{t} \in \mathbb{R}^{\mathbb{N}},\, \alpha \in \mathscr{J}, \tag{B.4}$$

except for finitely many factors all others are h_0, which equals unity, and the infinite product is really a finite one and well defined.

The space $\mathbb{R}^{\mathbb{N}}$ can be equipped with a Gaussian (product) measure (Hida et al., 1999; Holden et al., 1996; Janson, 1997; Malliavin, 1997), again denoted by Γ. Then the set $\{H_\alpha(\boldsymbol{t})/\sqrt{\alpha!} \,|\, \alpha \in \mathscr{J}\}$ is a CONS in $L_2(\mathbb{R}^{\mathbb{N}}, \Gamma)$ as the multivariate Hermite polynomials satisfy

$$\int_{\mathbb{R}^{\mathbb{N}}} H_\alpha(\boldsymbol{t})\,H_\beta(\boldsymbol{t})\,\Gamma(\mathrm{d}\boldsymbol{t}) = \alpha!\,\delta_{\alpha\beta}, \tag{B.5}$$

where the Kronecker symbol is extended to $\delta_{\alpha\beta} = 1$ in case $\alpha = \beta$ and zero otherwise.

C The Hermite Algebra

Consider first the usual univariate Hermite polynomials $\{h_k\}$ as defined in Appendix B, Eq. (B.1). As the univariate Hermite polynomials are a linear basis for the polynomial algebra, i.e. every polynomial can be written as linear combination of

Hermite polynomials, this is also the case for the product of two Hermite polynomials $h_k h_\ell$, which is clearly also a polynomial:

$$h_k(t)h_\ell(t) = \sum_{n=|k-\ell|}^{k+\ell} c_{k\ell}^{(n)} h_n(t) \tag{C.1}$$

The coefficients are only non-zero for integer $g = (k+\ell+n)/2 \in \mathbb{N}$ and if $g \geq k \wedge g \geq \ell \wedge g \geq n$ (Malliavin, 1997). They can be explicitly given

$$c_{k\ell}^{(n)} = \frac{k!\,\ell!}{(g-k)!\,(g-\ell)!\,(g-n)!}\,, \tag{C.2}$$

and are called the structure constants of the univariate Hermite algebra.

For the multivariate Hermite algebra, analogous statements hold Malliavin (1997):

$$H_\alpha(\boldsymbol{t})H_\beta(\boldsymbol{t}) = \sum_\gamma c_{\alpha\beta}^\gamma H_\gamma(\boldsymbol{t}). \tag{C.3}$$

with the multivariate structure constants

$$c_{\alpha\beta}^\gamma = \prod_{j=1}^{\infty} c_{\alpha_j\beta_j}^{\gamma_j}, \tag{C.4}$$

defined in terms of the univariate structure constants Eq. (C.2).

From this it is easy to see that

$$\mathbb{E}\left(H_\alpha H_\beta H_\gamma\right) = \mathbb{E}\left(H_\gamma \sum_\varepsilon c_{\alpha\beta}^\varepsilon H_\varepsilon\right) = c_{\alpha\beta}^\gamma \gamma!. \tag{C.5}$$

Products of more than two Hermite polynomials may be computed recursively, we here look at triple products as an example, using Eq. (C.3):

$$\begin{aligned} H_\alpha H_\beta H_\delta &= \left(\sum_\gamma c_{\alpha\beta}^\gamma H_\gamma\right) H_\delta \\ &= \sum_\varepsilon \left(\sum_\gamma c_{\gamma\delta}^\varepsilon c_{\alpha\beta}^\gamma\right) H_\varepsilon. \end{aligned} \tag{C.6}$$

D The Hermite Transform

A variant of the Hermite transform maps a random variable onto the set of expansion coefficients of the PCE (Holden et al., 1996). Any random variable $r \in L_2(\Omega)$ which may be represented with a PCE

$$r(\omega) = \sum_{\alpha \in \mathscr{J}} r^\alpha H_\alpha(\theta(\omega)) \tag{D.1}$$

is mapped onto

$$\mathscr{H}(r) := (r^\alpha)_{\alpha\in\mathscr{J}} =: (r) \in \mathbb{R}^{\mathscr{J}}. \tag{D.2}$$

This way $\bar{r} := \mathbb{E}(r) = r^0$ and $\mathscr{H}(\bar{r}) = (r^0, 0, 0, ...)$, as well as $\tilde{r}(\omega) := r(\omega) - \bar{r}$ and $\mathscr{H}(\tilde{r}) = (0, (r^\alpha)_{\alpha\in\mathscr{J},\alpha>0})$.

These sequences may be seen also as the coefficients of power series in infinitely many complex variables $z \in \mathbb{C}^{\mathbb{N}}$, namely by

$$\sum_{\alpha\in\mathscr{J}} r^\alpha z^\alpha,$$

where $z^\alpha := \prod_j z_j^{\alpha_j}$. This is the original definition of the Hermite transform (Holden et al., 1996).

It can be used to easily compute the Hermite transform of the ordinary product like in Eq. (C.3), as

$$\mathscr{H}(H_\alpha H_\beta) = (c_{\alpha\beta}^\gamma)_{\gamma\in\mathscr{J}}. \tag{D.3}$$

With the structure constants Eq. (C.4) one defines the matrices $Q_2^\gamma := (c_{\alpha\beta}^\gamma)$ with indices α and β. With this notation the Hermite transform of the product of two random variables $r_1(\omega) = \sum_{\alpha\in\mathscr{J}} r_1^\alpha H_\alpha(\theta)$ and $r_2(\omega) = \sum_{\beta\in\mathscr{J}} r_2^\beta H_\beta(\theta)$ is

$$\mathscr{H}(r_1 r_2) = \left((r_1) Q_2^\gamma (r_2)^T\right)_{\gamma\in\mathscr{J}}. \tag{D.4}$$

Each coefficient is a bilinear form in the coefficient sequences of the factors, and the collection of all those bilinear forms $\mathsf{Q}_2 = (Q_2^\gamma)_{\gamma\in\mathscr{J}}$ is a bilinear mapping that maps the coefficient sequences of r_1 and r_2 into the coefficient sequence of the product

$$\begin{aligned}\mathscr{H}(r_1 r_2) =: \mathsf{Q}_2((r_1),(r_2)) \\ = \mathsf{Q}_2\left(\mathscr{H}(r_1), \mathscr{H}(r_2)\right).\end{aligned} \tag{D.5}$$

Products of more than two random variables may now be defined recursively through the use of associativity. e.g. $r_1 r_2 r_3 r_4 = (((r_1 r_2) r_3) r_4)$:

$$\begin{aligned}\forall k > 2: \quad \mathscr{H}\left(\prod_{j=1}^k r_j\right) := \mathsf{Q}_k((r_1),(r_2),\ldots,(r_k)) := \\ \mathsf{Q}_{k-1}(\mathsf{Q}_2((r_1),(r_2)),(r_3)\ldots,(r_k)).\end{aligned} \tag{D.6}$$

Each Q_k is again composed of a sequence of k-linear forms $\{Q_k^\gamma\}_{\gamma\in\mathscr{J}}$, which define each coefficient of the Hermite transform of the k-fold product.

E Higher Order Moments

Consider RVs $\boldsymbol{r}_j(\omega) = \sum_{\alpha \in \mathscr{J}} \boldsymbol{r}_j^\alpha H_\alpha(\theta(\omega))$ with values in a vector space $\mathscr{V}$, then $\bar{\boldsymbol{r}}_j$, $\tilde{\boldsymbol{r}}_j(\omega)$, as well as $\boldsymbol{r}_j^\alpha$ are in $\mathscr{V}$. Any moment may be easily computed knowing the PCE. The k-th centred moment is defined as

$$\boldsymbol{M}^k_{\boldsymbol{r}_1 \dots \boldsymbol{r}_k} = \mathbb{E}\left(\otimes_{j=1}^k \tilde{\boldsymbol{r}}_j\right), \tag{E.1}$$

a tensor of order k. Thus it may be expressed via the PCE as

$$\boldsymbol{M}^k_{\boldsymbol{r}_1 \dots \boldsymbol{r}_k} = \sum_{\gamma^1, \dots, \gamma^k \neq 0} \mathbb{E}\left(\prod_{j=1}^k H_{\gamma^j}(\theta)\right) \otimes_{m=1}^k \boldsymbol{r}_m^{\gamma^m}, \tag{E.2}$$

and in particular:

$$\begin{aligned} \boldsymbol{C}_{\boldsymbol{r}_1 \boldsymbol{r}_2} &= \boldsymbol{M}^2_{\boldsymbol{r}_1 \boldsymbol{r}_2} = \mathbb{E}(\boldsymbol{r}_1 \otimes \boldsymbol{r}_2) \\ &= \sum_{\gamma, \beta > 0} \mathbb{E}\left(H_\gamma H_\beta\right) \boldsymbol{r}_1^\gamma \otimes \boldsymbol{r}_2^\beta \\ &= \sum_{\gamma > 0} \gamma! \, \boldsymbol{r}_1^\gamma \otimes \boldsymbol{r}_2^\gamma, \end{aligned} \tag{E.3}$$

as $\mathbb{E}\left(H_\gamma H_\beta\right) = \delta_{\gamma\beta}\gamma!$. The expected values of the products of Hermite polynomials in Eq. (E.2) may be computed analytically, by using the formulas from Appendix C.

References

Alspach, D. & Sorenson, H. (1972). Nonlinear Bayesian estimation using Gaussian sum approximations. *IEEE Transactions on Automatic Control*, *17*(4), 439–448.

Anderson, J. L. (2001). An ensemble adjustment Kalman filter for data assimilation. *Monthly Weather Review*, *129*, 2884–2903.

Arnst, M., Ghanem, R., & Soize, C. (2010). Identification of Bayesian posteriors for coefficients of chaos expansions. *Journal of Computational Physics*, *229*(9), 3134–3154.

Bader, B. W. & Kolda, T. G. (2006). Algorithm 862: MATLAB tensor classes for fast algorithm prototyping. *ACM Transactions on Mathematical Software*, *32*(4), 635–653.

Balakrishnan, S., Roy, A., Ierapetritou, M. G., Flach, G. P., & Georgopoulos, P. G. (2003). Uncertainty reduction and characterization for complex environmental fate and transport models: An empirical Bayesian framework incorporating the stochastic response surface method. *Water Resources Research*, *39*(12), 1350.

Bergemann, K., Gottwald, G., & Reich, S. (2009). Ensemble propagation and continuous matrix factorization algorithms. *Quarterly Journal of the Royal Meteorological Society*, *135*(643), 1560–1572.

Bishop, C. H., Etherton, B. J., & Majumdar, S. J. (2001). Adaptive sampling with the ensemble transform Kalman filter. Part I: Theoretical aspects. *Monthly Weather Review*, *129*(3), 420–436.

Blanchard, E. D. (2010). *Polynomial Chaos Approaches to Parameter Estimation and Control Design for Mechanical Systems with Uncertain Parameters*. PhD thesis, Department of Mechanical Engineering, VirginiaTech University.

Botev, Z. I., Grotowski, J. F., & Kroese, D. P. (2010). Kernel density estimation via diffusion. *Annals of Statistics*, *38*(5), 2916–2957.

Burgers, G., van Leeuwen, P. J., & Evensen, G. (1998). Analysis scheme in the ensemble Kalman filter. *Monthly Weather Review*, *126*, 1719–1724.

Christen, J. A. & Fox, C. (2005). MCMC using an approximation. *Journal of Computational and Graphical Statistics*, *14*(4), 795–810.

Engl, H. W., Hanke, M., & Neubauer, A. (2000). *Regularization of inverse problems*. Kluwer, Dordrecht.

Ephraim, Y. & Merhav, N. (2002). Hidden Markov processes. *IEEE Transactions on Information Theory*, *48*(6), 1518–1569.

Evensen, G. (1992). Using the extended Kalman filter with a multilayer quasi-geostrophic ocean model. *Journal of Geophysical Research*, *97*(C11), 17,905–17,924.

Evensen, G. (1994). Sequential data assimilation with a non-linear quasi-geostrophic model using Monte Carlo methods to forecast error statistics. *Journal of Geophysical Research*, *99*(C5), 10,143–10,162.

Evensen, G. (2003). The ensemble Kalman filter: theoretical formulation and practical implementation. *Ocean Dynamics*, *53*(4), 343–367.

Evensen, G. (2004). Sampling strategies and square root analysis schemes for the EnKF. *Ocean Dynamics*, *54*(6), 539–560.

Evensen, G. (2009a). *Data Assimilation — The Ensemble Kalman Filter*. Springer-Verlag, Berlin, 2^{nd} edition.

Evensen, G. (2009b). The ensemble Kalman filter for combined state and parameter estimation. *IEEE Control Systems Magazine*, *29*, 82–104.

Ghanem, R. & Spanos, P. D. (1991). *Stochastic finite elements — A spectral approach*. Springer-Verlag, Berlin.

Goldstein, M. & Wooff, D. (2007). *Bayes Linear Statistics - Theory and Methods*. Wiley Series in Probability and Statistics. John Wiley & Sons, Chichester.

Golub, G. H. & van Loan, C. F. (1996). *Matrix Computations*. Johns Hopkins University Press, Baltimore, 3^{rd} edition.

Gordon, N., Salmond, D., & Smith, A. (1993). Novel approach to nonlinear/non-Gaussian Bayesian state estimation. In *IEE Proceedings F Radar and Signal Processing*, volume 140, (pp. 107–113).

Hastings, W. K. (1970). Monte Carlo sampling methods using Markov chains and their applications. *Biometrika*, *57*(1), 97–109.

Hida, T., Kuo, H. H., Potthoff, J., & Streit, L. (1999). *White Noise-An Infinite Dimensional Calculus*. Kluwer, Dordrecht.

Holden, H., Øksendal, B., Ubøe, J., & Zhang, T.-S. (1996). *Stochastic Partial Differential Equations*. Basel: Birkhäuser Verlag.

Houtekamer, P. L. & Mitchell, H. L. (2001). A sequential ensemble Kalman filter for atmospheric data assimilation. *Monthly Weather Review*, *129*(1), 123–137.

Janson, S. (1997). *Gaussian Hilbert spaces*. Cambridge Tracts in Mathematics, 129. Cambridge University Press, Cambridge.

Jazwinski, A. H. (1970). *Stochastic Processes and Filtering Theory*. Academic Press, Inc., New York.

Julier, S. & Uhlmann, J. (2004). Unscented filtering and nonlinear estimation. *Proceedings of the IEEE*, *92*(3), 401–422.

Kučerová, A. & Matthies, H. G. (2010). Uncertainty updating in the description of heterogeneous materials. *Technische Mechanik*, *30*(1-3), 211–226.

Li, J. & Xiu, D. (2009). A generalized polynomial chaos based ensemble Kalman filter with high accuracy. *Journal of Computational Physics*, *228*(15), 5454–5469.

Lorenz, E. N. (1984). Irregularity: a fundamental property of the atmosphere. *Tellus A*, *36*(2), 98–110.

Lorenz, E. N. (2005). A look at some details of the growth of initial uncertainties. *Tellus A*, *57*(1), 1–11.

Luenberger, D. G. (1969). *Optimization by Vector Space Methods*. John Wiley & Sons, New York, London, Sydney, Toronto.

Ma, X. & Zabaras, N. (2009). An efficient Bayesian inference approach to inverse problems based on an adaptive sparse grid collocation method. *Inverse Problems*, *25*(3), 035013.

Malliavin, P. (1997). *Stochastic Analysis*. Springer: Springer-Verlag, Berlin.

Marzouk, Y. & Xiu, D. (2009). A stochastic collocation approach to Bayesian inference in inverse problems. *Communications in Computational Physics*, *6*(4), 826–847.

Marzouk, Y. M., Najm, H. N., & Rahn, L. A. (2007). Stochastic spectral methods for efficient Bayesian solution of inverse problems. *Journal of Computational Physics*, *224*(2), 560–586.

Matthies, H. G. (2005). Computational aspects of probability in non-linear mechanics. In A. Ibrahimbegović & B. Brank (Eds.), *Engineering Structures under Extreme Conditions. Multi-physics and multi-scale computer models in non-linear analysis and optimal design of engineering structures under extreme conditions*, volume 194 of *NATO Science Series III: Computer and System Sciences*. Amsterdam: IOS Press.

Matthies, H. G. (2007). *Encyclopedia of Computational Mechanics*, chapter Uncertainty Quantification with Stochastic Finite Elements. John Wiley & Sons, New York.

Matthies, H. G. (2008). Stochastic finite elements: Computational approaches to stochastic partial differential equations. *Zeitschrift für Angewandte Mathematik und Mechanik*, *88*(11), 849–873.

Pence, B., Fathy, H., & Stein, J. (2010). A maximum likelihood approach to recursive polynomial chaos parameter estimation. In *American Control Conference (ACC)*, (pp. 2144–2151).

Segal, I. E. & Kunze, R. A. (1978). *Integrals and Operators*. Springer-Verlag, Berlin.

Shen, C. Y., Evans, T. E., & Finette, S. (2010). Polynomial chaos quantification of the growth of uncertainty investigated with a Lorenz model. *Journal of Atmospheric and Oceanic Technology*, *27*(6), 1059–1071.

Skorokhod, A. V. (1982). *Studies in the Theory of Random Processes*. Dover Publications, New York.

Snyder, C., Bengtsson, T., Bickel, P., & Anderson, J. (2008). Obstacles to high-dimensional particle filtering. *Monthly Weather Review*, *136*(12), 4629–4640.

Stuart, A. M. (2010). Inverse problems: A Bayesian perspective. *Acta Numerica*, *19*, 451–559.

Tarantola, A. (2004). *Inverse Problem Theory and Methods for Model Parameter Estimation*. SIAM, Philadelphia.

Tippett, M. K., Anderson, J. L., & Bishop, C. H. (2003). Ensemble square root filters. *Monthly Weather Review*, *131*, 1485–1490.

Whitaker, J. S. & Hamill, T. M. (2002). Ensemble data assimilation without perturbed observations. *Monthly Weather Review*, *130*(7), 1913–1924.

Wiener, N. (1938). The homogeneous chaos. *American Journal of Mathematics*, *60*(4), 897–936.

Øksendal, B. (1998). *Stochastic Differential Equations, An Introduction with Applications*. Springer-Verlag, Berlin, 5^{th} edition.

Informatikberichte

2009-05	A. Rausch, U. Goltz, G. Engels, M. Goedicke, R. Reussner	LaZuSo 2009: 1. Workshop für langlebige und zukunftsfähige Softwaresysteme 2009
2009-06	T. Müller, M. Lochau, S. Detering, F. Saust, H. Garbers, L. Märtin, T. Form, U. Goltz	Umsetzung eines modellbasierten durchgängigen Enwicklungsprozesses für AUTOSAR-Systeme mit integrierter Qualitätssicherung
2009-07	M. Huhn, C. Knieke	Semantic Foundation and Validation of Live Activity Diagrams
2010-01	A. Litvinenko and H. G. Matthies	Sparse data formats and efficient numerical methods for uncertainties quantification in numerical aerodynamics
2010-02	D. Grunwald, M. Lochau, E. Börger, U. Goltz	An Abstract State Machine Model for the Generic Java Type System
2010-03	M. Krosche, R. Niekamp	Low-Rank Approximation in Spectral Stochastic Finite Element Method with Solution Space Adaption
2011-01	L. Märtin, M. Schatalov, C. Knieke	Entwicklung und Erweiterung einer Werkzeugkette im Kontext von IT-Ökosystemen
2011-02	B. V. Rosić, A. Litvinenko, O. Pajonk, H. G. Matthies	Direct Bayesian update of polynomial chaos representations
2011-03	H. G. Matthies	White Noise Analysis for Stochastic Partial Differential Equations
2011-04	O. Pajonk, B. V. Rosić, A. Litvinenko, H. G. Matthies	A Deterministic Filter for non-Gaussian Bayesian Estimation